The Performance Prediction of HD Gear Reducer in Industrial Robots using Machine Learning Approach

Kumar Shivam, Kai-Chieh Tsao, Jen-Chung Hsiao

***Abstract*— Harmonic drive reducers are essential components of industrial robot arms, primarily due to their high reduction ratios, concentric shafts, compact size, and low backlash, making them particularly suitable for small to medium load industrial robots. However, their intricate mechanical structure, coupled with low vibration characteristics, poses challenges in determining performance attributes. One common failure mode in harmonic drives is flex spline fatigue fracture, which requires specialized testing platforms and removal of harmonic drives for measuring torsional stiffness. To address these challenges, this study introduces a machine learning-based vibration analysis approach for the online prediction of performance attributes in harmonic drive reducers. An accelerated testbed is employed to simulate loading and operational conditions of harmonic drives in real robots. This testbed collects vibration data during operation and measures the torsional stiffness and transmission error of the harmonic drive. The collected vibration data is then processed using discrete wavelet transformation, followed by feature extraction from the transformed signals. These extracted features are used to train an artificial neural network designed to simultaneously predict the torsional stiffness coefficient, average transmission error, and the maximum transmission error. The mean squared error and mean absolute error of the proposed method are significantly lower, demonstrating the superiority of the proposed machine learning approach in addressing the challenges associated with evaluating and predicting the performance of harmonic drive reducers in industrial robots.**

Index Terms*— *Artificial neural networks, Discrete wavelet transforms, Feature extraction, Harmonic Drive Reducer, Vibrations.

I. Introduction

As the global industrial landscape advances towards Industry 4.0, the fusion of information technology with the manufacturing sector becomes indispensable for fostering industrial evolution and maintaining a competitive edge. The progression of intelligent manufacturing technologies, particularly the implementation of smart capabilities such as failure prediction and health monitoring in machinery, is vital for contemporary industrial growth. A key component in this context is the harmonic drive (HD) reducer, a unique gearbox mechanism consisting of three core elements: the circular spline, flex spline, and wave generator. HD reduces has several advantages such as compact size, high transmission efficiency, and minimal noise generation, HD reducers are ideally suited for a diverse range of applications, spanning the aerospace industry, medical equipment, and industrial robotics. In the realm of robot arms, harmonic drives play a pivotal role in articulated robots, where the health prognosis and diagnostic capabilities of these drives are crucial for ensuring operational efficiency, minimizing downtime, and enhancing the overall performance and longevity of industrial robotic systems.

Harmonic drive (HD) reducers offer numerous advantages over traditional reducers and gearboxes; however, their compact size and intricate design also render them susceptible to various failure modes. In the context of industrial robots, where HD reducers are subjected to high loading, continuous operation, and non-uniform torsional loads, some prevalent failure modes [1] include tooth wear, tooth cracking, flex spline cracking, fatigue failure, and excessive loading. While proper maintenance and load management can prevent some of these failure modes, others such as fatigue failure and flex spline failure can be spontaneous and challenging to detect. Additionally, progressive failures like tooth wear and lubrication aging contribute to the gradual degradation of HD reducer performance over time. Consequently, numerous studies in the field of HD reducers emphasize the detection, monitoring, and prognosis of these failure modes to ensure optimal performance and longevity of industrial robotic systems.

A considerable body of research is dedicated to assessing and analyzing the degradation of harmonic drive (HD) reducers using sophisticated time series data analysis techniques. One notable study [2] presents a performance degradation assessment (PDA) methodology, employing low-frequency time series data, including input-output speed, torque, gearbox temperature, and three-axis vibration, to establish a degradation model utilizing genetic programming. As these data-driven models typically necessitate comprehensive datasets, accelerated life test (ALT) benches, as exemplified in [3], are often employed to obtain the required data. ALT test benches [4]–[7] are instrumental in simulating the operational conditions of HD reducers, as well as measuring transmission error, torsional stiffness, and other essential performance indicators.

While a plethora of techniques exists for offline evaluation of HD reducer performance, vibration analysis remains the predominant method for online assessment tasks. The ease of installation for vibration sensors streamlines data collection.

This work was supported by the Ministry of Economic Affairs, R.O.C under Grant No. 108-EC-17-A-22-0171.

Kumar Shivam is currently employed as Project Manager at Automation and Robotics Division of Precision Machinery Research and Development Center, No. 27, Gongyequ 37th Rd, Xitun District, Taichung City, 407 Taiwan (R.O.C.) (Phone:05-2919925#6105, e-mail: e10725@mail.pmc.org.tw).

Kai-Chieh Tsao is currently employed as Department Manager at Automation and Robotics Division of Precision Machinery Research and Development Center, No. 27, Gongyequ 37th Rd, Xitun District, Taichung City, 407 Taiwan (R.O.C.) (Phone:05-2919925#8885, e-mail: e10505@mail.pmc.org.tw).

Jen-Chung Hsiao holds the position of Chief Technology Director in general manager office at Precision Machinery Research and Development Center, No. 27, Gongyequ 37th Rd, Xitun District, Taichung City, 407 Taiwan (R.O.C.) (Phone:04-23599009#768, e-mail: e8222@mail.pmc.org.tw).

Nevertheless, due to the low vibration characteristics inherent to HD drives, direct analysis of vibration data is not recommended. Consequently, numerous studies that focus on PDA and health prediction [8], [9] of gearboxes with low vibration employ advanced techniques such as discrete wavelet transformation (DWT). A variety of studies [10]–[15] propose that discrete wavelet transformation facilitates the extraction of valuable features from vibrational data. These decomposed signals can subsequently be processed using neural networks [16] and other modeling techniques [17], [18], thereby contributing to a more comprehensive and accurate prediction of HD reducer performance and health.

Artificial neural networks (ANN) have been extensively utilized in the realm of health monitoring, performance degradation assessment (PDA), and damage detection for gearboxes, owing to their data-driven nature and universal approximation capabilities. For instance, in [19], ANN is employed to detect damage in the planetary gearbox of a wind turbine, while in [20], ANN is used for identifying helicopter gearbox faults based on vibration data. ANN has proven to be effective for processing vibration data from various gearbox types [21], [22]. When combined with advanced preprocessing techniques, such as discrete wavelet transformation (DWT), the accuracy and reliability of ANN models for fault diagnosis can be significantly enhanced, as suggested in [16], [23], [24].

Convolutional neural networks (CNN), particularly the 1D CNN variant [25] , have also been applied to vibration-based prediction and classification tasks involving time-series data. The effectiveness of 1D CNN in fault diagnosis stems from its ability to efficiently extract features from time-series data and to fuse the features of multiple axes vibration data without the need for preprocessing [26]. Notably, 1D CNN models have demonstrated exceptional accuracy in fault diagnosis, detection tasks, and multi-axis vibration fusion, as evidenced in [27]–[32]. In terms of selecting between ANN and CNN models, there is no definitive set of rules dictating the appropriate model for specific applications. However, as gleaned from the literature reviewed above, both ANN and CNN models yield commendable accuracy when employed for PDA, fault diagnosis, and health monitoring tasks.

Building upon the existing body of knowledge, this study aims to develop a performance prediction model for harmonic drive (HD) reducers employed in industrial robot arms using machine learning techniques. To achieve this objective, an accelerated life test (ALT) bench is designed and implemented to simulate the operating conditions and facilitate the collection of vibration data, as detailed in Section II. Section III outlines the measurement techniques and key performance indicators used in this study, providing the necessary background information to contextualize the research findings. Subsequently, discrete wavelet transformation (DWT) and feature extraction are applied to the acquired vibration signals, as elaborated in Section IV. Two machine learning models, artificial neural networks (ANN) and convolutional neural networks (CNN), are employed for training and prediction tasks, as presented in Section V. The performance and prediction accuracy of both models are compared and discussed in Section VI, providing insights into their respective strengths and weaknesses in the context of HD reducer performance prediction. Finally, the study summarizes its findings and contributions in Section VII, emphasizing the implications of this research for improving the reliability and efficiency of industrial robot arms through the effective monitoring and prediction of HD reducer performance.

II. Accelerated Life Testing Platform

In this study, an ALT platform is designed to simulate the operating conditions of a robot arm equipped with a harmonic drive (HD) reducer. A specific HD reducer featuring a 1:80 reduction ratio is employed, as depicted in Fig. 1. The HD reducer comprises four key components: a wave generator, a flex spline, a circular spline, and a cross bearing. This particular reducer is manufactured by Shinewe Motors and bears the model number TCS-20-80-UT.

Fig. 1 The HD reducer used for accelerated life testing.

The working principle of the HD reducer involves the interaction of the aforementioned components. The wave generator, typically consisting of an elliptical cam, is mounted on the input shaft. As the wave generator rotates, it imparts an elastic deformation to the flex spline, which is a flexible, thin-walled cylindrical component with external teeth. This deformation, in turn, causes the flex spline to engage with the circular spline, a rigid, internally toothed component. Due to the difference in tooth count between the flex spline and the circular spline, a relative rotation occurs, resulting in a high reduction ratio. The cross bearing serves to support and stabilize the entire assembly, ensuring smooth operation and minimal backlash.

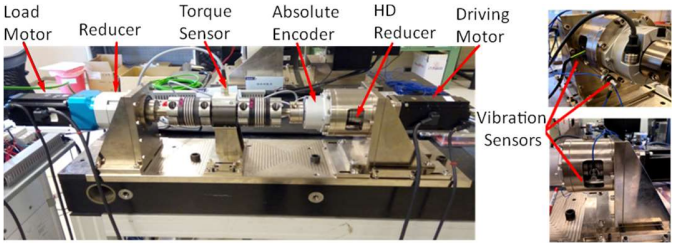

Fig. 2 The accelerated life testing platform.

Fig. 2 presents the image of the accelerated life test (ALT) platform utilized in this study. The platform comprises a 750W servo motor (Yaskawa SGM7J-08A7A6C), which supplies input torque to the harmonic drive (HD) reducer, securely positioned within the bracket. A high-precision absolute encoder (Heidenhain RCN 2510) featuring a system accuracy of ±2.5 arcseconds (arcsec) is employed to measure transmission accuracy. Centrally situated within the transmission chain is a torque transducer (HBM T22 100Nm) with a ±0.3% linear error and a maximum torque range of ±100 Nm. This component serves to measure the output torque of the HD reducer. At the end of the transmission line, a servo motor identical to the driving motor is paired with a planetary reducer with a 1:70

reduction ratio. This motor-reducer combination simulates the load on the HD reducer, replicating its operational conditions.

Three piezoelectric accelerometers are mounted on the three axes of the harmonic drive, as depicted in Fig. 3, while an additional sensor is installed on the z-axis of the motor, which represents the most dominant axis for motor vibration. The study employs a high-speed data acquisition module, the NI-9234 with NI-cDAQ-9181, from National Instruments to collect and process the data obtained from the sensors.

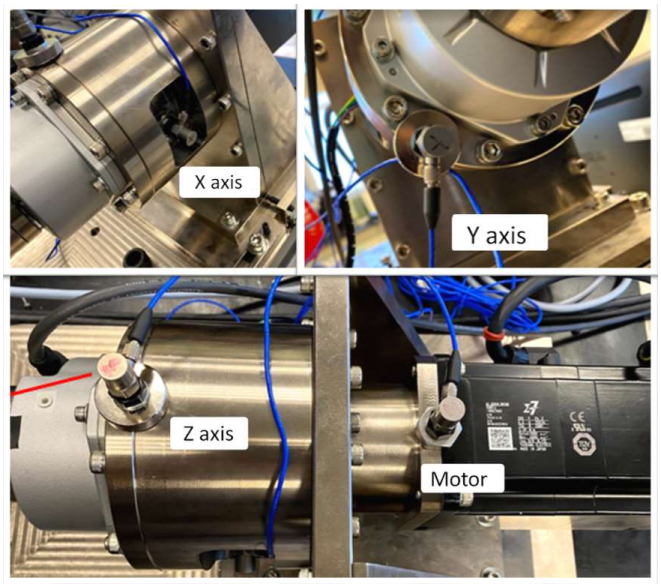

Fig. 3 Installation locations of piezoelectric vibration sensors.

III. PERFORMANCE INDICATORS OF HD REDUCER

The performance of HD reducers can be effectively evaluated using two key parameters: transmission accuracy [4] and torsional stiffness (K) [33]. Transmission accuracy serves as an essential metric for assessing the wear and tear experienced by the flex spline and circular spline teeth, as well as providing valuable information on the backlash occurring within the HD reducer. On the other hand, torsional stiffness represents the flex spline's ability to resist deformation when subjected to an external force while in a locked position. This parameter is particularly relevant for evaluating the structural integrity and durability of the HD reducer under various operational conditions. Moreover, torsional stiffness provides insights into the potential performance degradation of the HD reducer over time, which can inform maintenance decisions and ensure the longevity of the robotic system.

In this study, two types of transmission errors are calculated to assess the performance of the harmonic drive reducer: average transmission error (e_{avg}) and maximum transmission error (e_{max}). The harmonic drive is subjected to 360 rotations of one degree each on the ALT platform. The input position is measured using the input servo motor's encoder, while the output position is determined from the absolute encoder installed at the output shaft of the HD reducer.

The average transmission error (e_{avg}) is computed as the mean difference in position readings (shown in Equation 1) throughout the rotations, as illustrated in Equation 2. This metric provides insight into the general performance and accuracy of the HD reducer under normal operating conditions. On the other hand, the maximum transmission error (e_{max}) is calculated as the difference between the maximum positive direction error and the maximum negative direction error, as presented in Equation 2. This parameter is essential for determining the worst-case scenario in terms of transmission error and evaluating the reliability of the HD reducer under extreme conditions. A visual representation of the transmission error data gathered using the ALT platform is shown in Fig. 4. To enhance clarity, the transmission error unit has been converted to arcminutes (arcmin), where one arcmin is equal to 1/60th of a degree.

$$\Delta\theta = (\theta_{in} - \theta_{out}) \tag{1}$$

$$e_{avg} = \frac{1}{n}\sum_{i=0}^{n} \Delta\theta_i \tag{2}$$

$$e_{max} = \max(\Delta\theta_i) - \min(\Delta\theta_i) \ \ for\ i \in [0, n] \tag{3}$$

Where, θ_{in} is the input shaft position in degrees, θ_{out} is the output shaft position in degrees and n is total number of measurements in one cycle, i.e. 360 incremental rotations of 1 degree.

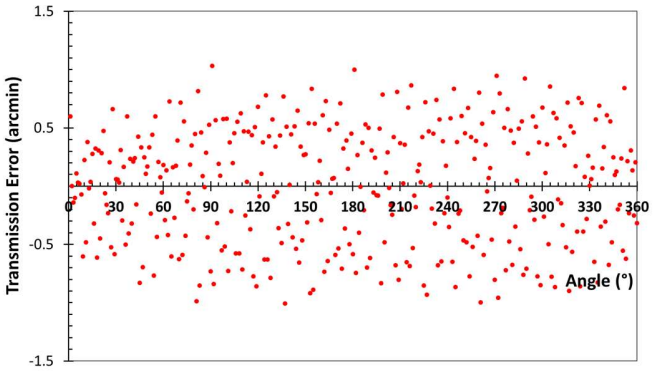

Fig. 4 Transmission error plot of the HD reducer gathered from ALT platform.

The torsional stiffness (K) of a HD reducer is determined using the hysteresis curve. To obtain the curve, the input shaft of the HD reducer is locked by applying brakes to the input motor. Subsequently, the loading motor applies torque, and the position of the output shaft is measured using the absolute encoder mounted on the output shaft. The resulting difference in the output shaft position relative to its initial position reflects the stiffness of the flex spline when subjected to an external load. Fig. 5 illustrates a hysteresis curve obtained from the ALT platform employed in this study.

Typically, torsional stiffness (K) is assessed through a three-step process, which involves dividing the hysteresis curve into distinct segments. Three torque (T) values specified by the manufacturer are utilized to design the hysteresis curve test. In the present study, the three values comprise T_1 at 7 Nm, T_2 at 25 Nm, and T_3 at 34 Nm. The K values corresponding to these three torque levels can be calculated using a piecewise linear approximation applied to the hysteresis curve, as demonstrated in Equation 4.

$$\begin{cases} K_1 = \dfrac{T_1}{\theta_1} \; if \; T \le T_1 \\ K_2 = \dfrac{T_2 - T_1}{\theta_2 - \theta_1} \; if \; T_1 < T \le T_2 \\ K_3 = \dfrac{T_3 - T_2}{\theta_3 - \theta_2} \; if \; T_2 < T \le T_3 \end{cases} \quad (4)$$

Where, where the torsional distortions of the flex spline at torques T_1, T_2 and T_3 is specified as θ_1, θ_2 and θ_3.

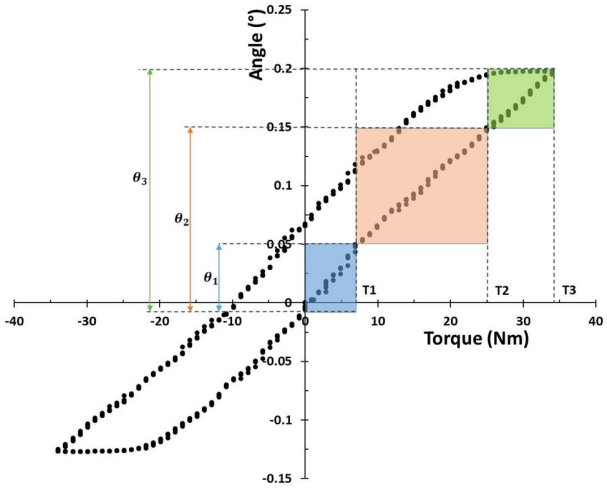

Fig. 5 The hysteresis curve of the HD reducer gathered from ALT platform.

The ALT test was conducted as follows: Initially, a 40 Nm load was applied using the loading torque and gear reducer, while the driving motor rotated the HD reducer at an input speed of 2400 RPM. The HD reducer is turned one full clockwise and then counterclockwise rotation, and the process is repeated, totally lasting for 30 minutes. Subsequently, a measurement cycle was executed by rotating the HD reducer 360° in a clockwise direction to collect vibration data from the three axes of the HD reducer and the driving motor's Z-axis. At the same time the torque output of the HD reducer was also measured and recorded using the torque transducer connected to the output shaft. Following this, the transmission errors and K values were measured as previously described in this section. In total, 3500 test cycles were performed, amounting to 1750 hours of accelerated life testing.

IV. Feature Extraction

In this study, a DWT-based preprocessing approach is employed for the analysis of vibration data obtained from the ALT platform. The DWT decomposes the original signal into distinct frequency components by selecting an appropriate wavelet function and applying the transformation function to break the signal into a high-frequency component (detail coefficient) and a low-frequency component (approximation coefficient). This decomposition process can be executed iteratively to divide the signal into multiple levels, as illustrated in Fig. 6.

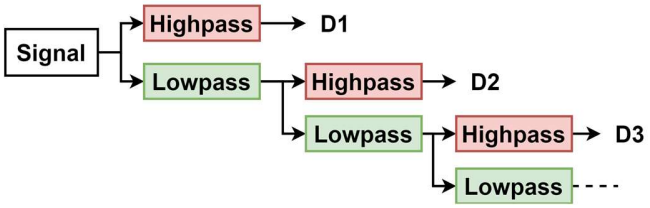

Fig. 6 The signal decomposition process of discrete wavelet transform.

Drawing from existing literature, the Symlet wavelet function [11], [14], [34] is chosen for the DWT task in this study, and a 7-level decomposition is performed on the vibration data, as depicted in Fig. 7. This choice of wavelet function and decomposition level is informed by previous research, which has demonstrated the effectiveness of this approach for analyzing vibration data in similar applications. In Fig. 7, the left column displays the low-frequency components of the original signal at the top, while the right column presents the high-frequency components corresponding to different levels of decomposition. This visual representation helps to illustrate the effectiveness of the DWT in decomposing the signal into its constituent frequency bands, enabling more detailed analysis of the vibration data.

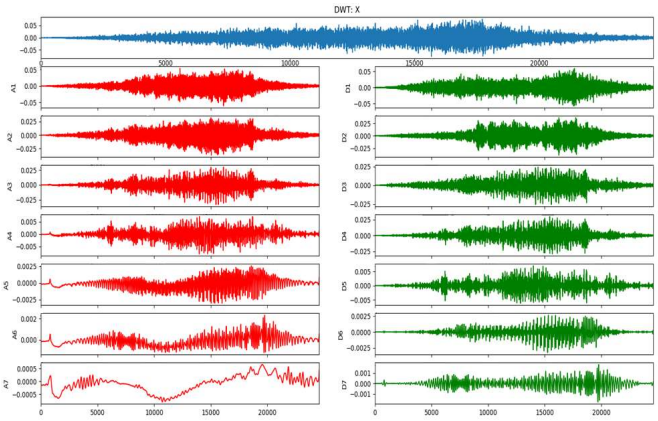

Fig. 7. The discrete wavelet transform of one sample of vibration data from X axis of the HD reducer.

Following the decomposition process, the low-frequency components of all 7 levels were selected, and feature extraction was performed using a Python programming language software library called TSFRESH [35]. A total of 20 features were extracted from the decomposed signal. Initially, statistical features such as mean, median, standard deviation, variance, percentile values, root mean square, mean of derivatives, zero-crossing rate, mean zero-crossing rate, and Shannon entropy value were calculated. Subsequently, time-series features, including autoregressive coefficients, absolute energy, auto-correlation, non-linearity statistics, time-series complexity, first location of maximum, largest fixed point of dynamics, mean change, and time reversal asymmetry statistics, were computed.

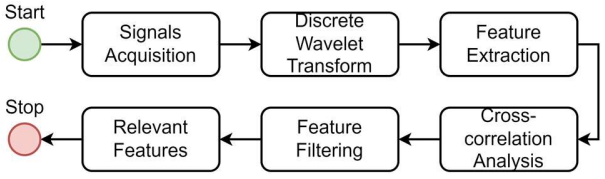

Fig. 8. Feature extraction and filtering process of vibration and torque signals.

As illustrated in Fig. 8, a smaller data set consisting of 500 signals was first utilized to extract the specified features. Thereafter, a cross-correlation analysis was conducted to identify features exhibiting high correlation with other features. A visual representation of the cross-correlation between features of different decomposed signals is presented in Fig. 9. Subsequently, a filtering function was applied to remove features displaying more than 75% correlation in either positive or negative directions. In this process, the study confirmed that the output torque features were highly correlated with the vibration features, and thus, they were discarded entirely. After the filtering process, a total of 204 relevant features were retained for further modeling tasks.

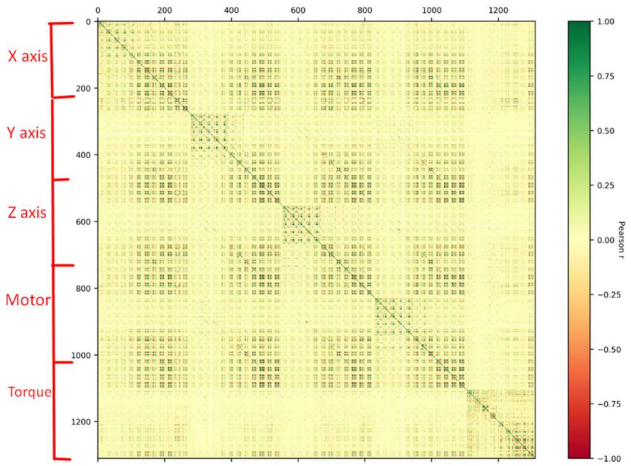

Fig. 9. Cross-correlation of various features extracted from harmonic drive three axes vibration, motor z axis vibration and output torque signal.

V. Machine Learning Models

In this study, the filtered features extracted in Section IV are employed to construct a machine learning training and prediction pipeline. Two machine learning approaches, namely, ANN and 1D CNN, were selected for comparison purposes. For a comprehensive understanding of the mathematical equations and further details on these machine learning methods, readers may refer to [36]. As depicted in Fig. 9, both approaches were designed as multi-input multi-output models. The raw signals underwent preprocessing using DWT, and the low-frequency components from the 7-level decompositions were utilized to calculate the relevant features. Subsequently, these features were employed to train ANN and 1D CNN models separately on 2,500 sets of vibration data. The remaining 1,000 sets were used for testing the performance of the two models. Both models were trained to predict maximum transmission error (e_{max}), average transmission error (e_{avg}), and torsional stiffness values of K2 and K3 simultaneously.

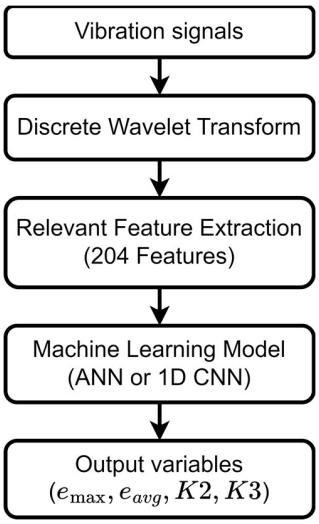

Fig. 10. Machine learning models training and prediction method and output variables.

ANN model used in this study was designed to have 4 hidden layers with 500, 500, 200 and 100 neurons respectively. Sigmoid activation function was applied to hidden layer's neurons. At last a linear activation layer was used as output layer with 4 neurons representing the 4 output variables of this study. The 1D CNN model employed in this study is comprised of several layers, each with distinct configurations and activation functions. The input layer, Layer 1, has a shape of (204, 1) and does not include an activation function. Layer 2, the first 1D CNN layer, consists of 128 filters, a kernel size of 6, a stride of 1, and utilizes the rectified linear unit (ReLU) activation function. Layer 3 is another 1D CNN layer with 64 filters, a kernel size of 3, a stride of 1, and the ReLU activation function. Layer 4 is a max-pooling layer with a pool size of 3 and a stride of 2. Layer 5, a 1D CNN layer, has 64 filters, a kernel size of 3, a stride of 1, and employs the ReLU activation function. Layer 6 is another max-pooling layer with a pool size of 3 and a stride of 2. Layer 7, a 1D CNN layer, is configured with 128 filters, a kernel size of 3, a stride of 1, and the ReLU activation function. Layer 8 is a global average pooling layer, while Layer 9 is a dense (hidden) layer containing 128 neurons and the ReLU activation function. Finally, Layer 10, the output layer, consists of 4 neurons with a linear activation function. Both models utilized mean absolute percentage error as the loss function and were trained for 1000 epochs using the ADAM optimizer to ensure consistency in the training process.

VI. Results

In order to compare the performance of ANN vs 1D CNN model, this study uses two metrics, normalized mean square error (NMSE) and mean absolute percentage error (MAPE) as shown in Equation 5 and Equation 6. Finally the overall accuracy of a model can be calculated as function of MAPE as shown in equation 7. In the equations below, $\hat{y}$ represents the predicted value, y is the actual/measured value and n is the total number of vibration dataset used for testing (1000 in this case). By examining these metrics, the study aims to provide a comprehensive analysis of the effectiveness and robustness of each method in estimating performance attributes of the HD reducer.

$$NMSE = \frac{\sum_{i=0}^{n}(y_i - \hat{y}_i)^2}{\sum_{i=0}^{n}(y_i)^2} \quad (5)$$

$$MAPE = \frac{\sum_{i=0}^{n}|y_i - \hat{y}_i|}{n} \times 100 \quad (6)$$

$$Accuracy = 100 - MAPE \quad (7)$$

TABLE I COMPARISON OF ANN AND CNN MODELS FOR PREDICTING THE PERFORMANCE INDICATORS OF HD REDUCER.

Output Variable	ANN NMSE	ANN MAPE	CNN NMSE	CNN MAPE
e_{max}	0.0121	7.57%	0.021	9.97%
e_{avg}	0.0001	0.63%	0.0002	0.89%
K2	0.0005	1.60%	0.0006	1.71%
K3	0.0012	2.12%	0.0024	3.31%
Model average	0.0035	2.98%	0.0061	3.97%

The Table 1 presents a comparison of the performance of the Artificial Neural Network ANN and 1D CNN models in predicting four output variables: maximum transmission error, average transmission error, torsional stiffness values K2 and K3. Across all output variables, the ANN model consistently outperformed the 1D CNN model, exhibiting lower NMSE and MAPE values, indicating better prediction accuracy. For instance, the ANN model achieved an NMSE of 0.0121 and a MAPE of 7.57% for e_{max}, while the CNN model had an NMSE of 0.021 and a MAPE of 9.97%. The average performance of the ANN model also surpassed that of the 1D CNN model, with an average NMSE of 0.0035 and MAPE of 2.98% compared to the 1D CNN model's average NMSE of 0.0061, MAPE of 3.97% and accuracy of 96.03%. This comparison highlights the superior performance of the ANN model for predicting the selected performance indicators in the context of HD reducer with 97.02% accuracy.

In Fig. 11, the ANN model's predictions for the entire dataset concerning e_{max} are depicted as a scatterplot with respect to the sample number. The figure shows that the model not only closely predicted the training set consisting of the initial 2500 samples but also accurately predicted the remaining 1000 samples used for testing. This consistent performance is similarly observed in the predictions for the other three output variables, as illustrated in Figs. 12, 13, and 14. For Figs. 11 and 12, the y-axis unit is arcmin, while for Figs. 13 and 14, the y-axis represents unitless *K2* and *K3* values. These results underscore the robustness and reliability of the ANN model in predicting the selected variables for both the training and testing datasets, emphasizing its potential for practical applications in HD reducer performance prediction.

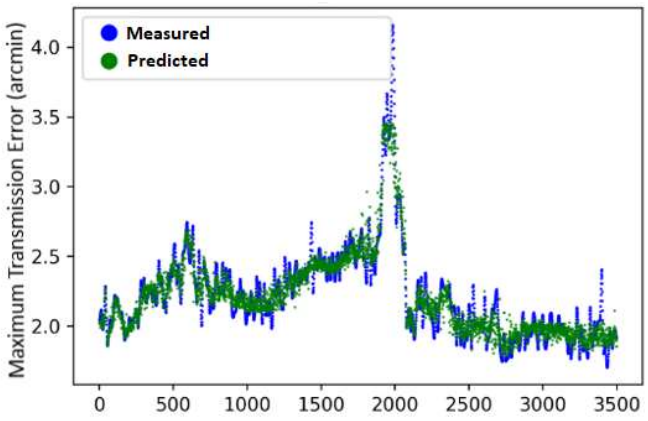

Fig. 11. Scatter plot comparison of measured vs predicted maximum transmission error for the ANN model.

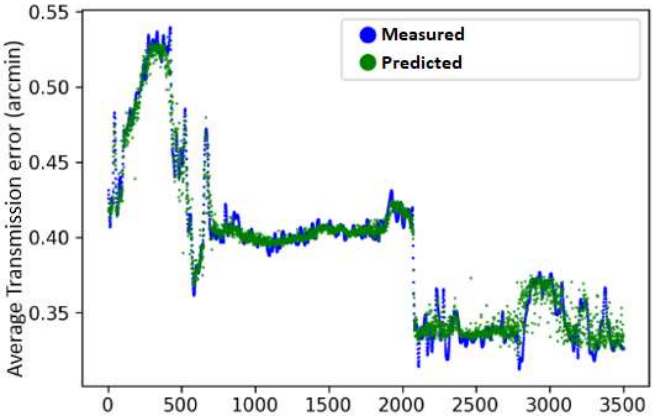

Fig. 12. Scatter plot comparison of measured vs predicted average transmission error for the ANN model.

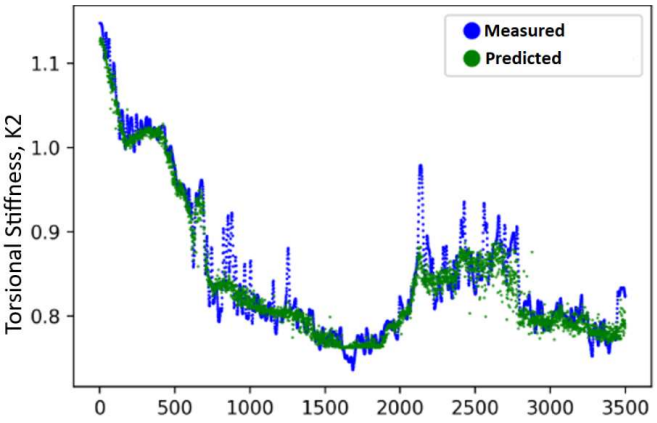

Fig. 13. Scatter plot comparison of measured vs predicted torsional stiffness *K2* for the ANN model.

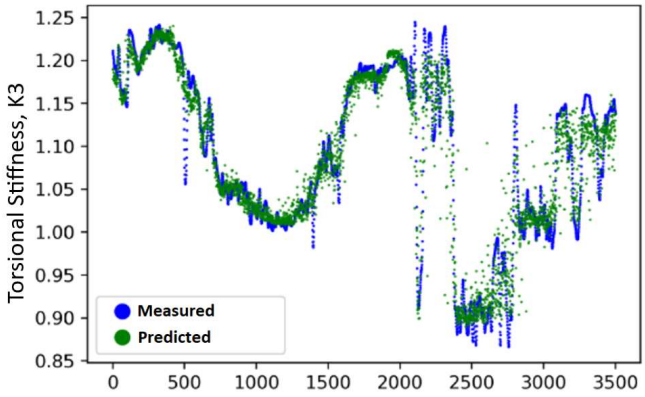

Fig. 14. Scatter plot comparison of measured vs predicted torsional stiffness *K3* for the ANN model.

VII. Conclusion

In conclusion, this study presents a performance prediction method of harmonic drive reducers using machine learning techniques. The study employed a DWT-based preprocessing approach to analyze vibration data and extract meaningful features using cross-correlation analysis, which were then utilized to train ANN and 1D CNN models for predicting key performance indicators such as maximum and average transmission errors and torsional stiffness values. The results demonstrated that the ANN model outperformed the 1D CNN model in terms of prediction accuracy, emphasizing the potential of the ANN model for practical applications in HD reducer performance prediction.

This research contributes to the existing body of knowledge by providing valuable insights into the performance prediction of HD reducers, as well as a reliable predictive model for monitoring and maintenance purposes. Future work could explore the integration of other advanced machine learning techniques, such as deep learning or ensemble methods, to further improve the predictive accuracy and robustness of the models. Additionally, incorporating real-time monitoring and control strategies based on the developed models could lead to more effective and proactive maintenance approaches, significantly reducing the downtime and costs associated with industrial robot arm failures.

References

[1] A. Raviola, A. De Martin, R. Guida, G. Jacazio, S. Mauro, and M. Sorli, "Harmonic Drive Gear Failures in Industrial Robots Applications: An Overview," in *Proceedings of the 6th European Conference of the Prognostics and Health Management Society*, 2021, pp. 350–360.

[2] T. Yan, Z. Bi, J. Liu, Y. Zhao, Y. Zhao, and D. Wang, "Performance degradation assessment methodology of harmonic reducer by using low-frequency time series data and genetic programming," *J. Phys. Conf. Ser.*, vol. 1983, no. 1, 2021.

[3] C. Zhang, S. Wang, Z. Wang, and X. Wang, "An accelerated life test model for harmonic drives under a segmental stress history and its parameter optimization," *Chinese J. Aeronaut.*, vol. 28, no. 6, pp. 1758–1765, 2015.

[4] B. S. Kim, S. T. Jeong, and H. J. Ahn, "The Prediction of the Angular Transmission Error of a Harmonic Drive by Measuring Noncontact Tooth Profile and Considering Three-dimensional Tooth Engagement," *Int. J. Precis. Eng. Manuf.*, vol. 24, no. 3, pp. 371–378, 2023.

[5] J. Zheng and W. Yang, "Failure Analysis of a Flexspline of Harmonic Gear Drive in STC Industrial Robot: Microstructure and Stress Distribution," *IOP Conf. Ser. Mater. Sci. Eng.*, vol. 452, no. 4, 2018.

[6] J. Y. Kuo, C. Y. Hsu, P. F. Wang, H. C. Lin, and Z. G. Nie, "Constructing Condition Monitoring Model of Harmonic Drive," *Appl. Sci.*, vol. 12, no. 19, pp. 1–13, 2022.

[7] B. Li, C. Qin, J. Tao, and C. Liu, "Failure Warning of Harmonic Reducer Based on Power Prediction," *J. Phys. Conf. Ser.*, vol. 2246, no. 1, 2022.

[8] J. Zhao, C. Gao, T. Tang, X. Xiao, M. Luo, and B. Yuan, "Overview of Equipment Health State Estimation and Remaining Life Prediction Methods," *Machines*, vol. 10, no. 6, 2022.

[9] Y. Yang, B. Yu, and W. Wang, "Research on equipment health prediction technology based on edge computing and VAE-TCN," *Procedia Comput. Sci.*, vol. 183, pp. 100–106, 2021.

[10] F. K. Omar and A. M. Gaouda, "Gearbox diagnostics using wavelet-based windowing technique," *J. Phys. Conf. Ser.*, vol. 181, no. 1, 2009.

[11] D. Strömbergsson, P. Marklund, K. Berglund, J. Saari, and A. Thomson, "Mother wavelet selection in the discrete wavelet transform for condition monitoring of wind turbine drivetrain bearings," *Wind Energy*, vol. 22, no. 11, pp. 1581–1592, 2019.

[12] R. Bajric, N. Zuber, G. A. Skrimpas, and N. Mijatovic, "Feature Extraction Using Discrete Wavelet Transform for Gear Fault Diagnosis of Wind Turbine Gearbox," *Shock Vib.*, vol. 2016, pp. 1–10, 2016.

[13] P. Kang, "Application of Wavelet Analysis to Condition Monitoring of Electromechanical Equipment," vol. 19, A. A. Petrosian and F. G. Meyer, Eds. Dordrecht: Springer Netherlands, 2001, pp. 501–541.

[14] N. B. Thamba, S. Venkata, Kiran Kamesh Thatikonda Nutakki, R. P. Duraiswamy, N. Mohammed, R. S. Wahab, R. V. Manglaraja, and A. V. Manivannan, "Fault analysis of worm gear box using symlets wavelet," *Arch. Acoust.*, vol. 45, no. 3, pp. 521–540, 2020.

[15] J. Da Wu and C. C. Hsu, "Fault gear identification using vibration signal with discrete wavelet transform technique and fuzzy-logic inference," *Expert Syst. Appl.*, vol. 36, no. 2 PART 2, pp. 3785–3794, 2009.

[16] M. Heydarzadeh, S. H. Kia, M. Nourani, H. Henao, and G.-A. Capolino, "Gear fault diagnosis using discrete wavelet transform and deep neural networks," in *IECON 2016 - 42nd Annual Conference of the IEEE Industrial Electronics Society*, 2016, pp. 1494–1500.

[17] A. H. Zamanian and A. Ohadi, "Gear fault diagnosis based on Gaussian correlation of vibrations signals and wavelet coefficients," *Appl. Soft Comput. J.*, vol. 11, no. 8, pp. 4807–4819, 2011.

[18] Z. Li, Z. Ma, Y. Liu, W. Teng, and R. Jiang, "Crack Fault Detection for a Gearbox Using Discrete Wavelet Transform and an Adaptive Resonance Theory Neural Network," *Strojniški Vestn. – J. Mech. Eng.*, vol. 61, no. 1, pp. 63–73, Jan. 2015.

[19] M. Strączkiewicz and T. Barszcz, "Application of artificial neural network for damage detection in planetary gearbox of wind turbine," *Shock Vib.*, vol. 2016, 2016.

[20] M. R. Dellomo, "Helicopter gearbox fault detection: A neural network based approach," *J. Vib. Acoust. Trans. ASME*, vol. 121, no. 3, pp. 265–272, 1999.

[21] Z. Chen, X. Chen, C. Li, R. V. Sanchez, and H. Qin, "Vibration-based gearbox fault diagnosis using deep neural networks," *J. Vibroengineering*, vol. 19, no. 4, pp. 2475–2496, 2017.

[22] R. C. Ümütlü, B. Hizarci, H. Ozturk, and Z. Kiral, "Classification of pitting fault levels in a worm gearbox using vibration visualization and ANN," *Sādhanā*, vol. 45, no. 1, p. 22, Dec. 2020.

[23] W. J. Staszewski and K. Worden, "Classification of faults in gearboxes - Pre-processing algorithms and neural networks," *Neural Comput. Appl.*, vol. 5, no. 3, pp. 160–183, 1997.

[24] M. Er-Raoudi, M. Diany, H. Aissaoui, and M. Mabrouki, "Gear fault detection using artificial neural networks with discrete wavelet transform and principal component analysis," *J. Mech. Eng. Sci.*, vol. 10, no. 2, pp. 2016–2029, 2016.

[25] S. Kiranyaz, O. Avci, O. Abdeljaber, T. Ince, M. Gabbouj, and D. J. Inman, "1D Convolutional Neural Networks and Applications: A Survey," pp. 1–20, 2019.

[26] J. C. Hsiao, K. Shivam, and T. Y. Kam, "Fault diagnosis method for worm gearbox using convolutional network and ensemble learning," in *Journal of Physics: Conference Series*, 2020, vol. 1509, no. 1.

[27] J. Chuya-Sumba, L. M. Alonso-Valerdi, and D. I. Ibarra-Zarate, "Deep-Learning Method Based on 1D Convolutional Neural Network for Intelligent Fault Diagnosis of Rotating Machines," *Appl. Sci.*, vol. 12, no. 4, pp. 1–16, 2022.
[28] F. Yu, L. Liao, K. Zhang, H. Xing, Q. Zhao, L. Zhang, and Z. Luo, "A Novel 1D-CNN-Based Diagnosis Method for a Rolling Bearing with Dual-Sensor Vibration Data Fusion," *Math. Probl. Eng.*, vol. 2022, 2022.
[29] C. C. Chen, Z. Liu, G. Yang, C. C. Wu, and Q. Ye, "An improved fault diagnosis using 1d-convolutional neural network model," *Electron.*, vol. 10, no. 1, pp. 1–19, 2021.
[30] P. Ong, Y. K. Tan, K. H. Lai, and C. K. Sia, "A deep convolutional neural network for vibration-based health-monitoring of rotating machinery," *Decis. Anal. J.*, vol. 7, no. February, p. 100219, 2023.
[31] Z. Jiang, Y. Lai, J. Zhang, H. Zhao, and Z. Mao, "Multi-factor operating condition recognition using 1D convolutional long short-term network," *Sensors (Switzerland)*, vol. 19, no. 24, 2019.
[32] T. Ince, S. Kiranyaz, L. Eren, M. Askar, and M. Gabbouj, "Real-Time Motor Fault Detection by 1-D Convolutional Neural Networks," *IEEE Trans. Ind. Electron.*, vol. 63, no. 11, pp. 7067–7075, 2016.
[33] A. Raviola, A. De Martin, and M. Sorli, "A Preliminary Experimental Study on the Effects of Wear on the Torsional Stiffness of Strain Wave Gears," *Actuators*, vol. 11, no. 11, p. 305, Oct. 2022.
[34] J. Rafiee, M. A. Rafiee, and P. W. Tse, "Application of mother wavelet functions for automatic gear and bearing fault diagnosis," *Expert Syst. Appl.*, vol. 37, no. 6, pp. 4568–4579, 2010.
[35] M. Christ, N. Braun, J. Neuffer, and A. W. Kempa-Liehr, "Time Series FeatuRe Extraction on basis of Scalable Hypothesis tests (tsfresh – A Python package)," *Neurocomputing*, vol. 307, pp. 72–77, 2018.
[36] K. Shivam, J. C. Tzou, and S. C. Wu, "Multi-step short-term wind speed prediction using a residual dilated causal convolutional network with nonlinear attention," *Energies*, vol. 13, no. 7, 2020.

Kumar Shivam, Ph.D., received his PhD. degree in mechanical and energy engineering from Kun Shan University, Tainan City, Taiwan, in 2020. Since 2018, he has been a Research Engineer and currently holds the position of Project Manager at the Intelligent Automation and Robotics Division of Precision Machinery Research & Development Center, Taichung City, Taiwan. His research interests encompass machine learning techniques, time series forecasting methods, hybrid learning algorithms, application of meta-heuristic algorithms, energy conservation in industrial robotics, and hybrid energy systems.

Kai-Chieh Tsao, received his Master's degree in mechanical engineering from National Yunlin University of Science and Technology, Yunlin, Taiwan. He currently holds the position of Department Manager at the Intelligent Automation and Robotics Division of Precision Machinery Research & Development Center, Taichung City, Taiwan. His research interests encompass machine design and automation systems.

Jen-Chung Hsiao, Ph.D., received the Ph.D. degree in mechanical engineering from National Chiao Tung University, Taiwan, in 2020. From 2012 to 2020, he was a Division Director of the Robotics & Automation Division. Since 2020, he has been a Chief Technology Director in general manager office, Precision Machinery Research & Development Center, Taichung City, Taiwan. His research interests include mechanical design optimization, reliability engineering, and robot calibration.